



# Pan-cancer analysis identifies protein arginine methyltransferases *PRMT1* and *PRMT5* and their related signatures as markers associated with prognosis, immune profile, and therapeutic response in lung adenocarcinoma

Jia Wang<sup>a,b,1</sup>, Meng Wu<sup>b,1</sup>, Jujie Sun<sup>c,1</sup>, Minxin Chen<sup>b,d</sup>, Zengfu Zhang<sup>b</sup>, Jinming Yu<sup>b,\*\*</sup>, Dawei Chen<sup>b,\*</sup>

<sup>a</sup> Shantou University Medical College, Shantou, 515041, Guangdong Province, China

<sup>b</sup> Department of Radiation Oncology and Shandong Provincial Key Laboratory of Radiation Oncology, Shandong Cancer Hospital and Institute, Shandong First Medical University and Shandong Academy of Medical Sciences, 250117, Jinan, Shandong Province, China

<sup>c</sup> Department of Pathology, Shandong Cancer Hospital and Institute, Shandong First Medical University and Shandong Academy of Medical Sciences, 250117, Jinan, Shandong Province, China

<sup>d</sup> Department of Oncology, The Affiliated Hospital of Southwest Medical University, Luzhou, Sichuan, China

## ARTICLE INFO

### Keywords:

*PRMT1*

*PRMT5*

Prognosis

Tumor immune microenvironment

Type I interferon pathway

Radiotherapy

## ABSTRACT

**Purpose:** Protein arginine methyltransferases (PRMTs) regulate several signal transduction pathways involved in cancer progression. Recently, it has been reported that PRMTs are closely related to anti-tumor immunity; however, the underlying mechanisms have yet to be studied in lung adenocarcinoma (LUAD). In this study, we focused on PRMT1 and PRMT5, key members of the PRMT family. And their signatures in lung carcinoma associated with prognosis, immune profile, and therapeutic response including immunotherapy and radiotherapy were explored.

**Methods:** To understand the function of PRMT1 and PRMT5 in tumor cells, we examined the association between the expression of PRMT1 and PRMT5 and the clinical, genomic, and immune characteristics, as well as the sensitivity to immunotherapy and radiotherapy. Specifically, our investigation focused on the role of PRMT1 and PRMT5 in tumor progression, with particular emphasis on interferon-stimulated genes (ISGs) and the pathway of type I interferon. Furthermore, the influence of proliferation, migration, and invasion ability was investigated based on the expression of PRMT1 and PRMT5 in human lung adenocarcinoma cell lines.

**Results:** Through the examination of receiver operating characteristic (ROC) and survival studies, PRMT1 and PRMT5 were identified as potential biomarkers for the diagnosis and prognosis. Additionally, heightened expression of PRMT1 or PRMT5 was associated with immunosuppressive microenvironments. Furthermore, a positive correlation was observed between the presence of PRMT1 or PRMT5 with microsatellite instability, tumor mutational burden, and neoantigens in the majority of cancers. Moreover, the predictive potential of PRMT1 or PRMT5 in individuals undergoing immunotherapy has been acknowledged. Our study ultimately revealed that the inhibition of PRMT1 and PRMT5 in lung adenocarcinoma resulted in the activation of the cGAS-

\* Corresponding author.

\*\* Corresponding author.

E-mail addresses: [sdyujinming@163.com](mailto:sdyujinming@163.com) (J. Yu), [dave0505@yeah.net](mailto:dave0505@yeah.net) (D. Chen).

<sup>1</sup> These authors contributed equally to this work.

STING pathway, especially after radiation. Favorable prognosis was observed in lung adenocarcinoma patients receiving radiotherapy with reduced PRMT1 or PRMT5 expression. It was also found that the expression of PRMT1 and PRMT5 influenced proliferation, migration, and invasion of human lung adenocarcinoma cell lines.

**Conclusion:** The findings indicate that PRMT1 and PRMT5 exhibit potential as immune-related biomarkers for the diagnosis and prognosis of cancer. Furthermore, these biomarkers could be therapeutically targeted to augment the efficacy of immunotherapy and radiotherapy in lung adenocarcinoma.

## 1. Introduction

Lung cancer is a prevalent form of malignancy and a prominent reason about relating cancer fatalities worldwide. Lung adenocarcinoma (LUAD) represents the highest incidence in all observed subtypes of lung carcinomas, accounting for approximately 85% of non-small cell lung cancer cases [1]. Despite significant advancements in immunotherapy, the long-term survival outcomes for individuals diagnosed with LUAD remain unsatisfactory [2]. Radiotherapy is an important means of treatment of non-small cell lung cancer, but the effectiveness of radiotherapy also needs to be improved. Consequently, the development of efficacious therapeutic targets and the exploring of precise diagnostic biomarkers and for immunotherapy and radiotherapy are imperative in order to extend the survival duration of LUAD patients.

Protein arginine methyltransferases (PRMTs) are a protein enzymes family and their main function are related to methyl arginine residues. PRMTs have been implicated in the proliferation and progression of tumors [3,4]. Their involvement encompasses epigenetic modifications during transcription, RNA processing, signal transduction, and diverse processes related to cancer-immunity. The implementation of immunotherapy has brought about a substantial transformation in cancer treatment, leading to notable improvements in overall survival (OS) rates and the quality of life experienced by patients. Research studies have consistently demonstrated a robust association between arginine and the anti-cancer immune response, thereby implying its pivotal role in modulating the effectiveness of immunotherapy [5–8].

The PRMTs methylarginine product is categorized into 3 primary types according the ultimate structure of the methylarginine [9]. Type I PRMTs, such as PRMT1, PRMT2, PRMT3, PRMT4, PRMT6, and PRMT8, facilitate the formation of mono-methylarginine (MMA) and asymmetric dimethylarginine (ADMA). Type II PRMTs, including PRMT5 and PRMT9, catalyze the formation of MMA and symmetric dimethylarginine (SDMA). Type III, represented by PRMT7, exclusively generates MMA [4]. Notably, PRMT1 and PRMT5 serve as molecular representatives of the PRMT family. The generation of methylarginine in mammalian cells is primarily attributed to PRMT1, accounting for more than 85%–90% of its production, while PRMT5 represents subtype II PRMTs [4,8]. Consequently, this study focuses on the investigation of PRMT1 and PRMT5.

The current body of research on the pathogenic mechanisms of PRMTs in LUAD, as well as their impact on the tumor immune microenvironment, is insufficient. Therefore, we undertook a comprehensive investigation employing multi-omics integration, validation of clinical data, and *in vitro* experimental validation. Specifically, we associated the gene expression levels of PRMT1 or PRMT5 with their diagnostic and prognostic significance in various cancers, with a particular focus on LUAD. The expression of PRMT1 and PRMT5 was correlated to immune cell infiltration, along with other immune-related markers through a comprehensive analysis encompassing various types of cancer. Given the established role of type I interferon (IFN) in enhancing the susceptibility of cancer cells to chemotherapy and radiotherapy [10–14], our investigation specifically focused on evaluating the prognosis of patients with LUAD who underwent radiotherapy. Consequently, the outcome of this research is to enhance our comprehension of PRMT genes and identify potential therapeutic targets for tumor immunotherapy and radiotherapy, especially in lung adenocarcinoma.

## 2. Materials and methods

### 2.1. Gene expression analysis of PRMT genes

The raw data was acquired from the TCGA database and GTEx database [15]. Statistical analyses were performed using R 4.3.0, which facilitated data transformation and normalization. Data visualization was conducted using the R package “ggplot2”. Immunofluorescence data obtained from the HPA (<http://www.proteinatlas.org>) were utilized to ascertain the distribution and subcellular localization of PRMT proteins, including PRMT1 and PRMT5.

### 2.2. Cell culture and qRT-PCR

MC38 was obtained from the laboratory of L.-F. Deng. Human bronchial epithelial cells (HBE), human adenocarcinoma cell lines (A549, H1299, and H1975), murine lung cancer cell lines (LLC and CMT167), murine lung epithelium (MCA-12), and 293T cells were purchased from the Cell Bank of the Chinese Academy of Sciences (Beijing, China). All cells were cultured in Dulbecco's Modified Eagle's medium (DMEM) (catalog no. C1995500BT) supplemented with 10% fetal bovine serum (FBS) (Gibco, catalog no. 10270-106, Brazil) and 1% penicillin/streptomycin (catalog no. P1400) at 37 °C in a humidified environment with 5% CO<sub>2</sub>. Mouse *Prmt1* and *Prmt5* knockdown lentiviruses plasmid, mouse *Prmt1* and *Prmt5* overexpression lentiviruses plasmid, and human PRMT1 and PRMT5

overexpression lentiviruses plasmid were purchased from miaolingbio (Wuhan, China), and the target sequences of *Prmt1* and *Prmt5* were designed and listed in Table S1.

Prior to infection, the virus produced through transfection of 293T cells was added to each well the cells were seed before. Following 3 days incubation, the cells successfully transfected were selected utilized 2  $\mu\text{g}/\text{mL}$  puromycin. siRNA targeting human PRMT1 and PRMT5, and mouse *Prmt1* and *Prmt5* were procured from Universal Biology (Anhui, China). After overnight cell seeding, siRNA was transfected into the cells, and the subsequent *in-vitro* experiments were conducted 48–60 h later.

The extraction and purification of total RNA were conducted using TRIzol Reagent (Tiangen, Beijing, China, catalog no.15596018). qRT-PCR was performed by using a QuantStudio 6 and 7 Pro Real-Time PCR System and a 384-well block with the SYBR Green Master Mix (Vazyme, Nanjing, China, catalog no.027E2242JA). The mRNA expression levels were normalized against  $\beta$ -actin using the change in the cycling threshold ( $\Delta$  Ct). The primers were designed by PrimerBank (<https://pga.mgh.harvard.edu/primerbank/>) and listed in Table S1, too.

### 2.3. Western blotting

The pretreated cells were collected and lysed using a cell lysis buffer for western blotting, following a prior washing step with cold phosphate-buffered saline (Beyotime Biotechnology; catalog no. P0013). Protein samples were analyzed using assay kits for BCA protein quantification (Beyotime Biotechnology, catalog no. P0012). The protein was subsequently loaded onto SDS-PAGE gels, then electrophoresed, and transferred onto polyvinylidene difluoride membranes (Millipore, catalogue no. IPVH00005). The primary antibodies were then incubated overnight. The following primary antibodies were obtained from Santa Cruz Biotechnology: anti-PRMT1 (B2) (catalog no. sc-166963), anti-PRMT5 (A11) (catalog no. sc-376937), anti-PRMT7 (E-9) (catalog no. sc-376077); anti- $\beta$ -actin (catalog no. 81115-1-RR) were obtained from Proteintech (Wuhan, China); anti-TBK1 (catalog no. 38066S), anti-phospho-TBK1 (catalog no. 5483S), anti-STING (catalog no. 13647), anti-phospho-STING (catalog no. 72971), and anti-STAT1 (catalog no. 9172) were purchased from Cell Signaling Technology (Massachusetts, America). The secondary antibodies were then incubated for 30 min. Then ECL was added, the membranes were exposed.

### 2.4. Flow cytometry and plate clone formation assay

The assessment of cells, both irradiated with a dose of 15Gy and those without irradiation, was conducted by flow cytometry with FITC-Annexin V (Vazyme, Nanjing, China, catalog no. A213-01/02), with the staining reagents diluted in accordance with the manufacturer's instructions. To determine cellular activity and proliferation, a plate clone formation assay was employed. Specifically, 1000 cells were exposed to a gradient of radiation doses ranging from 0 Gy to 6 Gy. The cells were cultured for 2 weeks and then fixed and stained.

### 2.5. Cell counting kit-8 analysis, the scratch wound assay and transwell invasion assay

To assess the proliferation ability of cells, CCK8 analysis was conducted. Specifically, every well introduced 1000 cells. And the blank group served as a control without any cells. The mixture of CCK8 solution and culture medium was added to the wells of cells and incubated at a temperature of 37 °C with 2 h. To calculate cell survival/proliferation, we subtracted the optical density (OD) values of the blank wells from that of the test wells using microplate readers.

In order to conduct scratch wound assays, a total of  $2 \times 10^5$  cells were plated until confluence was achieved. The detachment of cells from the monolayer was addressed by scratching it using a tip and subsequently washing it. To assess tumor cell migration, all cells were photographed 24 or 36 h after the wounding process depending on the degree of cell growth.

For the transwell invasion assay, the base of the chamber with 8  $\mu\text{m}$  pore filters (Corning) is preloaded with matrigel. Then, a suspension of  $2 \times 10^4$  cells per well was prepared in a 2% FBS medium and then seeded into the upper chamber. After 48 h, the upper chambers were removed from a 10% FBS medium from the bottom 24-well and washed, with the cells fixed and stained.

### 2.6. Diagnostic Prediction and clinical correlation analysis of PRMT1 and PRMT5

With the “pROC” R package, the receiver operating characteristic (ROC) of PRMT genes was determined in various malignancies. AUC values were categorized from 0.5 to 0.7, 0.7 to 0.9, and 0.9 to 1.0, indicating low, medium, and high predictive effects, respectively. The List of Abbreviations provides a comprehensive list of the 33 cancer species utilized in the TCGA database. Gene expression and clinical raw data were extracted from the TCGA (<https://portal.gdc.com>) dataset. In univariate Cox regression analysis, we calculated the probability (p) of each variable, the hazard ratio (HR), and the 95% confidence interval (CI) with the R package “forestplot”.

### 2.7. Clinical characteristics associated with PRMT1 and PRMT5 expression

RNA-Seq data from the TCGA database were converted to fragments per kilobase of exon per million mapped fragments and logarithmically transformed. The clinical characteristics were extracted from clinical raw data and analyzed. Chi-square tests were used to calculate p-values. By using ROC analysis and the “rms” package, LUAD and LUSC were visualized using a nomogram correlation model. The accuracy of the nomogram model was evaluated by examining calibration curves for patients with LUAD and LUSC

over the first, fifth, and ten years of their survival. The Nomogram correlation model was employed to visualize the relationship between LUAD and LUSC with ROC analysis and the “rms” package. A nomogram model was constructed to estimate the 1-year, 5-year, and 10-year overall survival (OS) for patients with LUAD and LUSC, and calibration curves were examined to assess its accuracy.

2.8. Genetic alteration analysis of PRMT1 and PRMT5

The mutational characteristics of PRMT1 and PRMT5, including multimodal cancer genomics data, were analyzed by the cBioPortal platform [16]. Genetic modifications were investigated by employing a rapid selection tool to input PRMT genes. This facilitated the acquisition of mutation sites and three-dimensional (3D) structures through the utilization of the “Mutations” module.

2.9. Immune-related characteristics of PRMT1 and PRMT5

An investigation of the relationship between PRMT1, PRMT5 expression and CD8<sup>+</sup> T cell infiltration and cancer-associated fibroblasts (CAF) in diverse cancer types was conducted by the TIMER 2.0 web server. Based on TCGA database somatic data, mutational burdens and microsatellite instability scores were calculated for each cancer. Neoantigen analyses were conducted using datasets from BEST ([https://rookietopia.com/app\\_direct/BEST/](https://rookietopia.com/app_direct/BEST/)). Additionally, the association between PRMT1 and PRMT5 expression and indicators of the tumor immune microenvironment, such as antigen presentation, immunostimulatory factors, chemokine expression, and receptor expression were analyzed in LUAD datasets including TCGA and multiple GEO datasets. We analyzed multiple immunotherapy GEO datasets and clinical information. Survival curves were drawn based on PRMT1 and PRMT5 expression.

2.10. The potential biological function of PRMT1 and PRMT5 in LUAD

The analysis of PRMT1 and PRMT5 expression in LUAD was conducted using the BEST datasets ([https://rookietopia.com/app\\_](https://rookietopia.com/app_)

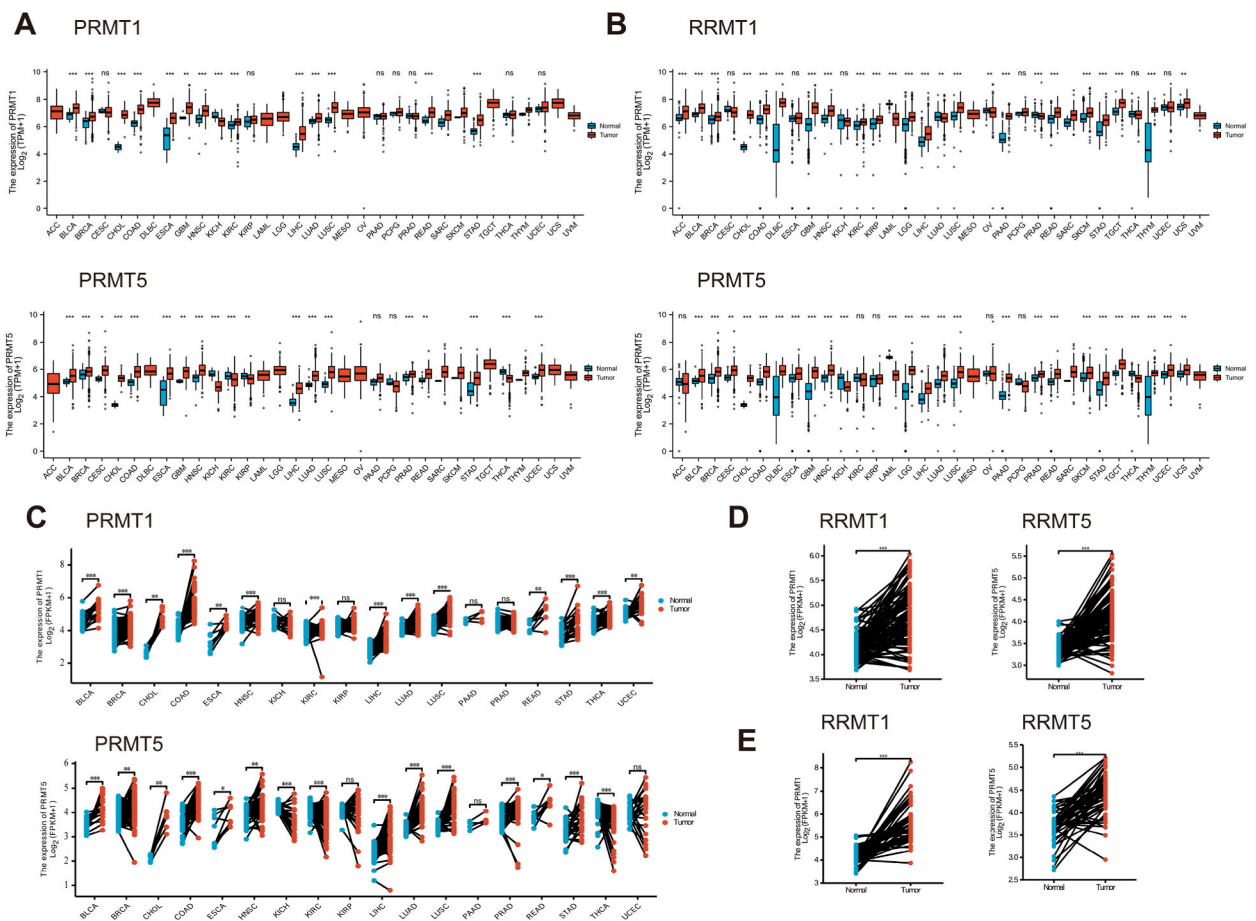


**Fig. 1.** Normal and tumor-derived PRMT1 and PRMT5 mRNA expression A, from TCGA database. B, from GTEx database and TCGA database. C, from TCGA datasets by pairwise comparisons. D, normal tissues vs lung cancer, E, vs colorectal cancer. ns, p > 0.05. \*p < 0.05; \*\*p < 0.01; \*\*\*p < 0.01.

direct/BEST/) and KEGG. Interferon stimulating genes (ISGs) were extracted and categorized into two groups based on gene expression levels of PRMT1 or PRMT5. The expression of ISGs in both groups was quantified to assess potential statistical differences. Additionally, survival curves were generated using the Kaplan-Meier Plotter. These curves were based on the gene expression data obtained from 70 lung cancer radiotherapy-treated patients.

### 2.11. CancerSEA analysis

CancerSEA was utilized to explore the roles of PRMT1 and PRMT5 in non-small cell lung cancer (NSCLC), with a particular focus on lung adenocarcinoma (LUAD) [17]. CancerSEA enables the decoding of various functional states of cancer cells at a single-cell level. To ensure robustness, we applied a filtering criterion of correlation strengths >0.1 and false discovery rates (FDRs) > 0.05 by employing a cor-based filtering approach on the single-cell datasets.

### 2.12. Correlation analyses among PRMT1 and PRMT5 expression with type I interferon pathway

Data of 33 cancer types was downloaded by R package ‘TCGAbiolinker’. The signature genes of type I IFN response are obtained from The Molecular Signatures Database (MSigDB; <http://software.broadinstitute.org/gsea/msigdb/>). These genes included *Zbp1*, *Mx2*, *Mx1*, *Cxcl11*, *Ifi44*, *Cxcl9*, *Oas2*, *Ifnb1*, *Ccl4*, *Irgm2*, *Oasl2*, *Ifit1b1*, *Irf7*, *Ifna4*, *Isg15*, *Oasl1*, *Ifit1b1*, *Cxcl10*, *Ifitm6*, *Ccl5*, *Irgm1*, *Stat2*, *Stat1*, *Irf9*, *Irf8*, *Adar*, *Nlrc5*, *Ifitm3*, *Samhd1*, *Myd88*, *Trim56*, *Trim6*, and *Shmt2*. The GSVA scores of the type I interferon response in each TCGA tumor sample were evaluated to calculate the Spearman correlation with PRMT1 or PRMT5 expression.

### 2.13. Statistical analysis

Using the Kruskal-Wallis test, gene expression levels were compared between tumors and normal tissues, and between cancer cells was compared by Wilcoxon rank sum test. All aforementioned R packages were executed using R software version 4.3.0, with statistical significance determined at  $p < 0.05$ .

## 3. Results

### 3.1. Pan-cancer gene expression analysis of PRMT1 and PRMT5

The PRMT gene mRNA expression levels were examined in tumors and surrounding normal tissues from TCGA and found to be significantly higher in most cases (Fig. 1A, S1A). Furthermore, TCGA and GTEx databases for the expression of PRMT genes were evaluated, too (Fig. 1B). Based on TCGA datasets, PRMT gene expression was significantly higher in almost all cancer types according to paired comparisons (Fig. 1C). Cross-validation study compared the PRMT1 and PRMT5 mRNA expression levels in TCGA human lung cancer, colorectal cancer, and corresponding normal tissues. In tumor tissues, PRMT genes were both significantly expressed

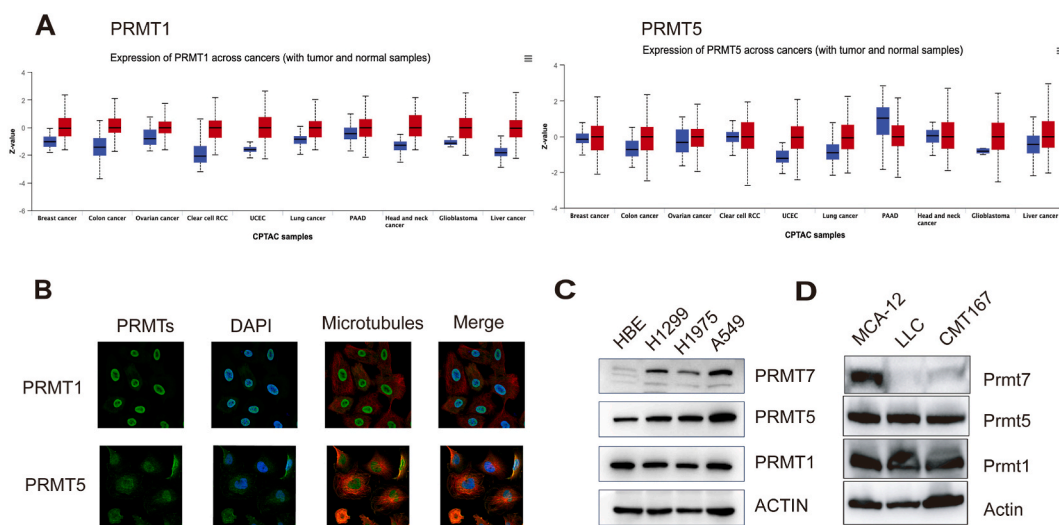


**Fig. 2.** Protein expression, intracellular localization, and western blotting validation of PRMT1 and PRMT5. **A** Protein expression level of PRMT1 and PRMT5. **B** The immunofluorescence labeling from HPA database. **C** Western blotting results in human lung cancer cell lines (H1299, H1975 and A549) and normal human lung cells HBE. **D** Western blotting results in murine lung carcinoma cell lines (LLC and CMT167) and normal murine lung cell MCA-12. Representative data are shown from 2 independent experiments. Identification of the diagnostic and prognostic value of PRMT1 and PRMT5.

(Fig. 1D and E).

3.2. PRMT1 and PRMT5 protein expression, intracellular localization, and westernblotting validation

From the UALCAN database, PRMT protein expression was found to be significantly elevated in most cancer types (Fig. 2A, S2A), which is consistent with PRMT mRNA levels [17,18]. To determine the intracellular localization of PRMT1 and PRMT5, we examined the subcellular distribution of PRMT1 in A549 cells (human lung adenocarcinoma cell line) and PRMT5 in U-251 (human brain glioma cells) by immunofluorescence staining of microtubules and the nucleus (DAPI) from HPA database. According to Fig. 2B, PRMT1 colocalized with DAPI-labeled nuclei, indicating that it is subcellularly located in the nuclei. Colocalization with DAPI-labeled nuclei and microtubules indicated PRMT5's subcellular localization in the nucleus and cytoplasm (Fig. 2B, S2B). For asymmetric demethylation, PRMT1, a type-I PRMT, is the primary enzyme. PRMT5, a type-II PRMT, is critical, too. There is only one PRMT molecule type-III that produces MMA, PRMT7. In comparison with the normal HBE, which served as a control, PRMT5, and PRMT7 protein levels were significantly elevated in human lung cancer cell lines, including H1299, H1975 and A549. The expression of PRMT1 in

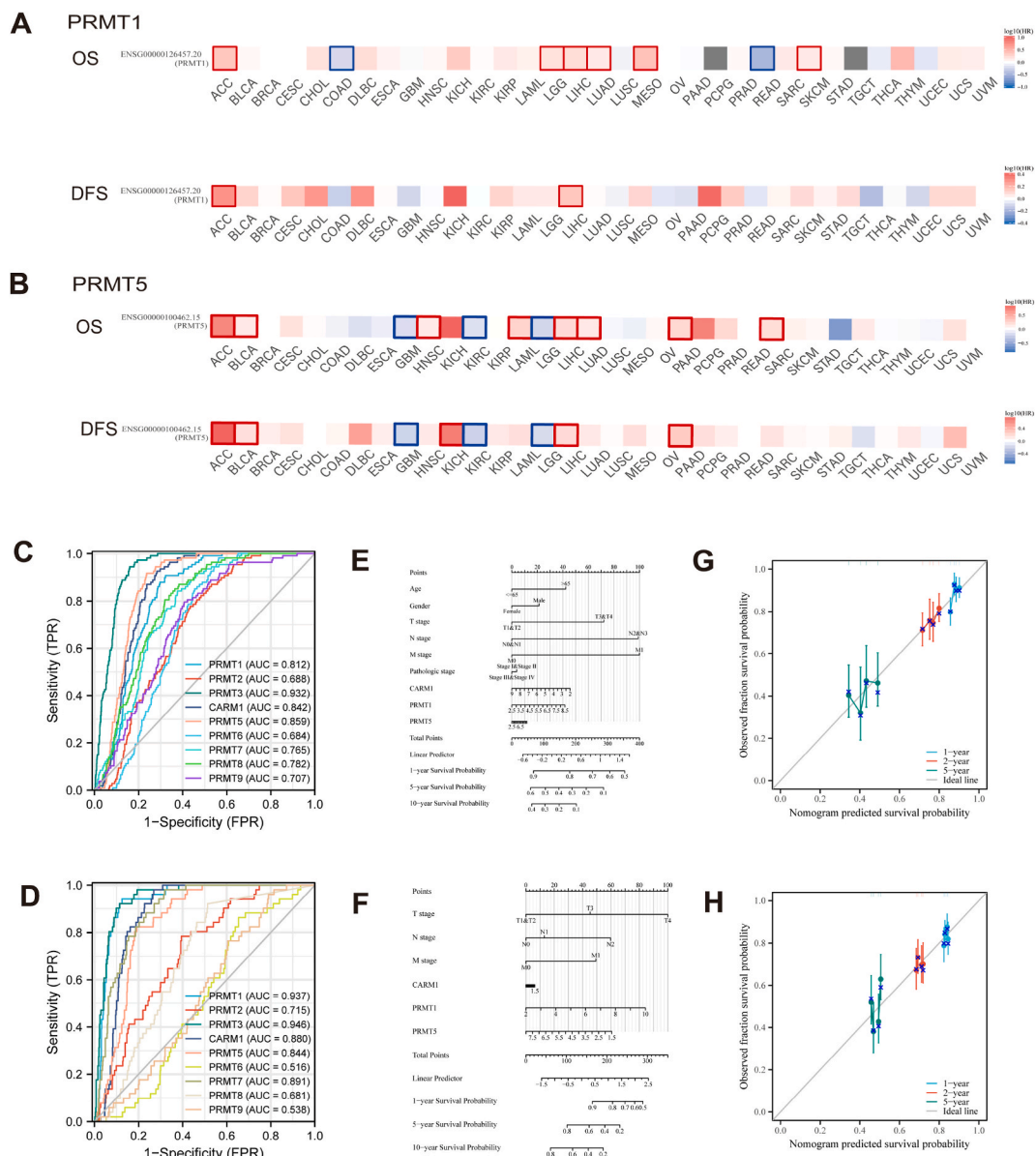


Fig. 3. Identifying PRMT1 and PRMT5 prognostic values. Correlation between A, PRMT1 and B, PRMT5 mRNA expression level and patient OS and DFS from TCGA database. Red borders represent high expression predicting poor prognosis, while blue borders indicate the opposite. C–D, the ROC analysis, E–F, the Nomogram correlation model as well as G–H, the calibration curve of the nomogram for LUAD and LUSC were listed.

H1299 and H1975 has indeed not increased compared with that in HBE, however, was higher than that of PRMT7 in Fig. 2C. Murine lung cancer cells, on the other hand, expressed little PRMT7 protein (Fig. 2D). Therefore, we chose PRMT1 and PRMT5 in human lung cancer cell lines as representative molecules of the PRMT family for subsequent validation.

Diagnostic values of RRMT and PRMT5 were confirmed using the AUC, and when the AUC was greater than 0.8, it was considered to be predictive of tumor occurrence. 12 types of cancer were highly (AUC >0.8) predicted by PRMT1 expression, such as BLCA (AUC = 0.820), CHOL (AUC = 1.000), COAD (AUC = 0.939), DLBC (AUC = 0.818), ESAD (AUC = 0.961), ESCA (AUC = 0.921), LAML (AUC = 0.990), LIHC (AUC = 0.917), LUSC (AUC = 0.953), PADD (AUC = 0.957), READ (AUC = 0.915), and TGAT (AUC = 0.829) (Fig. S3). AUC >0.8 was also able to accurately predict the diagnosis of 17 different cancers based on PRMT5 expression: CHOL (AUC = 1.000), COAD (AUC = 0.850), DLBC (AUC = 0.864), ESAD (AUC = 0.885), ESCA (AUC = 0.860), GBM (AUC = 0.923), KICH (AUC = 0.930), LAML (AUC = 1.000), LGG (AUC = 0.951), LICH (AUC = 0.839), LUAD (AUC = 0.888), LUSC (AUC = 0.917), PAAD (AUC = 0.956), READ (AUC = 0.825), TGCT (AUC = 0.845), THCA (AUC = 0.854), and THYM (AUC = 0.834) (Fig. S4).

Patients with cancer were evaluated for their OS and DFS based on PRMT1 and PRMT5 expression. It was found that there was a significant reduction of overall survival time among patients with ACC, LGG, LIHC, LUAD, MESO, and SARC whose PRMT1 expression was elevated. The high expression of PRMT1 in ACC and LICH patients is a poor prognostic indicator of disease-free survival (Fig. 3A).

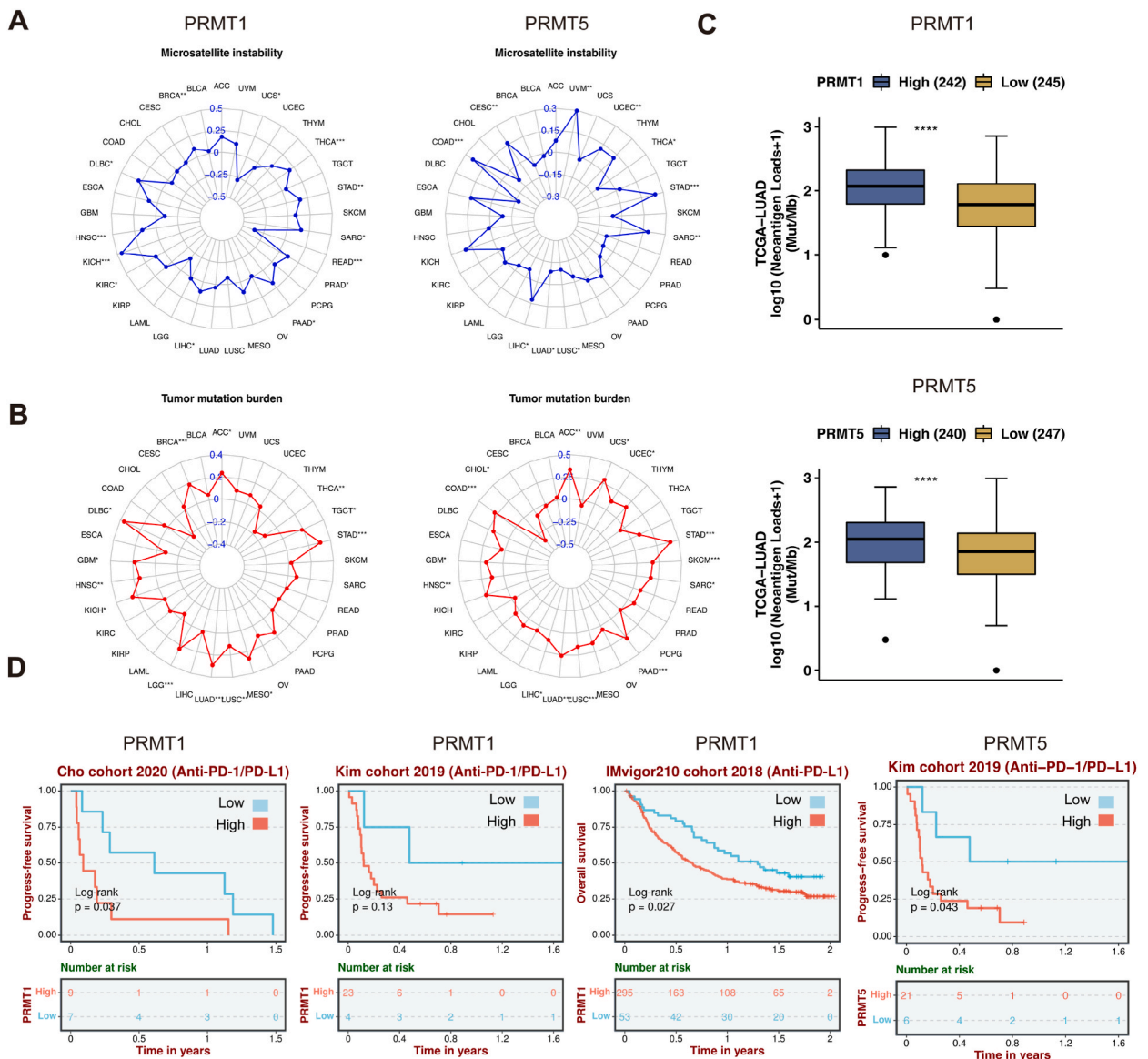


Fig. 4. PRMT1 and PRMT5 immunological characteristics. A–C, The correlation analysis of PRMT1 and PRMT5 expression level with A, MSI, B, TMB, and C, the neoaigen loads. D, The relevance between PRMT1 and PRMT5 expression levels and immune checkpoint blockade treatments such as anti-PD-L1 and anti-PD-1 treatment from GEO database. ns,  $p > 0.05$ ; \*\*\*\* $p < 0.0001$ .

In patients with ACC, HNSC, LAML, LIHC, LUAD, PAAD, and SARC, PRMT5 expression exerts adverse effects on prognosis (Fig. 3B). Univariate Cox regression was used to analyze the p-values, hazard ratios (HR), and confidence intervals of PRMT1 and PRMT5 expression in multiple tumors. Accordingly, PRMT1 and PRMT5 expression were closely associated with poorer prognosis in numerous malignancies, particularly LUAD (Fig. S5). This result was confirmed by multiple LUAD datasets obtained from the GEO database (Fig. S6). As shown in Fig. 3C–D, PRMT1 and PRMT5 provided high diagnostic and prognostic values for LUAD and LUSC, respectively. Since risk scores and prognosis are highly correlated, we incorporated clinical parameters into nomogram correlation analysis for LUAD and LUSC. Utilizing this nomogram, we estimated first-, fifth-, and ten-year survival rates for LUAD and LUSC patients (Fig. 3E–F). In order to demonstrate the accuracy of the nomogram, calibrating curves were performed in patients with LUAD and LUSC (Fig. 3G–H). In the first-, fifth-, and ten-year OS nomograms, accuracy was high, median, and low, respectively. A high correlation was found between the expression of PRMT1 and PRMT5 and lung cancer survival, particularly in LUAD.

### 3.3. Clinical characteristics associated with PRMT1 and PRMT5 expression

The clinical characteristics of LUAD associated with PRMT1 and PRMT5 were investigated. As shown in Table S2 and Table S3, expression levels of PRMT1 and PRMT5, as well as clinical and pathological characteristics were shown in lung cancer patients. Several clinical features were significantly correlated with PRMT1 expression level, such as T stage, N stage, pathologic stage, gender, anatomic neoplasm subdivision2 (including central and peripheral lung), number of pack-years smoked, smoker status, OS event, and median number pack-years smoked (IQR). A significant association was also found between PRMT5 expression level and most clinical characteristics including T stage, M stage, pathologic stage, gender, residual tumor, smoker, OS event and DSS event. Subsequent univariate and multivariate Cox regression analyses revealed that PRMT5 expression was independently predictive of OS and DFS in patients with lung cancer (Table S4, S5). Results indicated that PRMT1 and PRMT5 expression was highly predictive of lung cancer patient survival.

### 3.4. Genetic alteration analysis of PRMT1 and PRMT5

It was examined whether PRMT mutations are present in various tumor tissues using the cBioPortal database. In Fig. S6, mutations in the PRMT gene related to multiple malignancies were examined, including mutations, structural variants, amplifications, deep deletions, and multiple mutations. An illustration of PRMT1 and PRMT5 mutation types, locations, and associated domains was depicted in Fig. S7, along with a 3D model of the PRMT proteins with mutations mapped.

### 3.5. Immune-related characteristics of PRMT1 and PRMT5

A critical determinant for the outcome of tumor immunotherapy is the tumor immune microenvironment (TIME). According to Fig. S8A, PRMT1 and PRMT5 expression was positively correlated with CAF infiltration in most cancers, whereas a negative correlation was found between the two genes expression and CD8<sup>+</sup> T cell in TIME (Fig. S8B). Based on the TIMER 2.0 database, we found correlations between PRMT1 and PRMT5 and CD8<sup>+</sup> T cells, MDSC cells, NK cells, and CAF in lung adenocarcinoma (Fig. S9). Negative correlations were found between high PRMT1 or PRMT5 expression and immune-activating CD8<sup>+</sup> T cells and NK cells; positive correlations were found with MDSC and CAF expression, which represent an inhibitory immune microenvironment. Based on the ssGSEA algorithm, PRMT1 and PRMT5 are highly expressed in TCGA human LUAD and SKCM, indicating low CD8<sup>+</sup> T cell or cytotoxic cell infiltration (Figs. S8C–D).

Additionally, we performed a correlation analysis between the expression of PRMT1 and PRMT5 and the amount of MSI, TMB, and neoantigen loads. In most cancers (Fig. 4A–C), PRMT1 and PRMT5 expression were significantly positively correlated with MSI, TMB, and neoantigens. Additionally, we discovered that PRMT1 and PRMT5 expression correlated negatively with antigen presentation, immune stimulators, chemokines, and receptor expression in most LUAD datasets, including TCGA and multiple GEO datasets such as GSE41271, GSE72094, GSE26939, GSE42127, GSE50081, GSE31210, GSE3141, GSE19188, GSE68465, GSE68571, and GSE8894 (Fig. S10). PRMT1 and PRMT5 can contribute to immune-suppressive microenvironments, while the inhibition of PRMT1 or PRMT5 expression could improve the efficacy of immunotherapy.

A poor response to immunotherapy is largely due to an immunosuppressive microenvironment that leads to uncontrollable tumor growth, progression, and metastasis [19,20]. A microenvironment that is immunosuppressive may be associated with the expression of PRMT1 and PRMT5, making them potential therapeutic targets for tumor immunotherapy. In a subsequent study, we investigated the possible relationship between PRMT1 or PRMT5 expression and the efficacy of immune checkpoint therapies such as anti-PD-L1 or anti-PD-1. LUAD immunotherapy datasets including IMvigor210, Kim cohort 2019, and Cho cohort 2020 all showed poor immunotherapy efficacy when PRMT1 and PRMT5 expression was high (Fig. 4D). PRMT1 and PRMT5 expression appeared to be negatively correlated with LUAD immunotherapy efficacy, suggesting they are potential targets for improving LUAD immunotherapy.

### 3.6. Identification of the potential biological function of PRMT1 and PRMT5 in LUAD

Further study of the mechanisms underlying PRMT expression and tumor immunity was conducted. In LUAD, KEGG analyses of PRMT1 and PRMT5 expression revealed that both genes are involved in cell growth, death, and replication and repair, transcription, and translation pathways (Figs. S11–12). It was consistent with previous findings showing that PRMT1 and PRMT5 expression were significantly positive correlates of MSI, TMB, and neoantigen load. We analyzed single-cell expression of PRMT1 and PRMT5 in NSCLC,



**Fig. 5.** PRMT1 and PRMT5 confer radio-sensitization through the IFN-I pathway. A–B, Correlation between A PRMT1 or B PRMT5 expression with ISGs expression in LUAD from TCGA database. C, the *Prmt1* and *Prmt5* MC38 knockdown cell qRT-PCR validation. D, the PRMT1 or PRMT5 knockdown MC38 cell validation. E, qRT-PCR results of *Ifnb1* and *Cxcl10*. F, *p*-TBK1 expression in *Prmt1* or *Prmt5* overexpressed MC38 tumor cells. G, The effects of *prmt1* and *prmt5* on radiotherapy induced cell death *in vitro*, including flow cytometry with FITC-Annexin V and H, Radiotherapy plate clone formation assay. I, *p*-TBK1 expression in si-*Prmt1* and si-*Prmt5* MC38 tumor cells with or without IR. \* $p < 0.05$ ; \*\* $p < 0.01$ ; \*\*\* $p < 0.001$ ; \*\*\*\* $p < 0.0001$ .

particularly LUAD, using the single-cell database CancerSEA in order to investigate their function at the single-cell level. It was found that PRMT1 positively correlated with cell cycle, DNA repair, and DNA damage, but negatively correlated with metastasis, inflammation, angiogenesis, and senescence in NSCLC [21] (Fig. S13A). In LUAD, positive correlations with DNA damage, cell cycle, EMT, DNA repair, metastasis, and expansion were found [22] (Fig. S13B). Angiogenesis and inflammation were negatively correlated with PRMT5, while cell cycle and DNA damage were positively correlated (Fig. S13C) [21]. Both PRMT1 and PRMT5 expression were negatively correlated with inflammatory pathways in NSCLC single-cell data, which is consistent with our database analysis.

PRMT1 expression in LUAD was enriched for the cytosolic DNA-sensing pathway according to KEGG analysis (Fig. S11). An activation of the cytosolic DNA-sensing pathway or cGAS-STING pathway leads to an interferon-I response, which is crucial for tumor immunity induced by radiation therapy. The expression of genes associated with ISGs in LUAD was examined, and most patients with low expression of PRMT1 and PRMT5 had significantly high expression of ISGs, indicating that the expression of PRMT1 and PRMT5 is closely related to the IFN-I response (Fig. 5A, B). As reported in the literatures, MC38 cell line is a necessary tool line used to study the mechanism of type I interferon response [23–25]. Therefore, knockdown MC38 cell lines of PRMT1 or PRMT5 were established next (Fig. 5C, D). As shown in Fig. 5E, lower PRMT1 or PRMT5 expression resulted in enhanced ISG expression, including *Ifnb1* and *Cxcl10*. The qRT-PCR results were consistent with the data analysis in Fig. 5A and B. Meanwhile, overexpression of *Prmt1* or *Prmt5* in MC38 tumor cells showed reduced activation of the type I interferon pathway (Fig. 5F). We performed flow cytometry with FITC-Annexin V and plate clone formation assays to examine the impact of PRMT1 and PRMT5 on radiotherapy-induced cell death *in vitro*. As revealed by apoptotic flow cytometry, after 96 h of radiotherapy, there was a greater proportion of apoptotic cells with PRMT1 or PRMT5 knockdown cells compared to the group that did receive radiotherapy (Fig. 5G). Plate clone formation assay results showed that knockdown of PRMT1 or PRMT5 sensitized radiotherapy (Fig. 5H), consistent with flow cytometry results. The above results indicate that knockdown of *prmt1* or *prmt5* can increase the proportion of necrotic apoptotic cells in tumor cells. It has been reported in the literature that radiation induces the strong activation of the cGAS-STING pathway through the circular enhancement of necrotic apoptosis and the activation of the cGAS-STING pathway to stimulate radiotherapy anti-tumor immunity [23,25]. The results of western blotting showed that the type I interferon pathway was strongly activated after radiotherapy in tumor cells that knocked down *prmt1* or *prmt5* (Fig. 5I).

Further substantiating PRMT1 and PRMT5 involvement in human lung adenocarcinoma (LUAD), PRMT1 or PRMT5 in H1299 and H1975 human lung adenocarcinoma cells with siRNA was silenced. Western blotting revealed an upregulation of *p*-TBK1, indicating a significantly enhanced type I interferon response in LUAD after transient suppression of PRMT1 or PRMT5, respectively (Fig. 6A). Meanwhile, overexpression of PRMT1 or PRMT5 in LUAD tumor cell lines showed reduced activation of the type I interferon pathway (Fig. 6B). This outcome is completely consistent with the results of our database analyses and knockdown and overexpression MC38 cell line experiments in Fig. 5. In TCGA pan-cancer cohorts, PRMT1 or PRMT5 were negatively associated with type I interferon response in a variety of tumors (Fig. 6C), especially LUAD (Fig. 6D), with statistical significance. The results of western blotting showed that deficiency of intracellular PRMT1 or PRMT5 strongly activated the cGAS-STING pathway (Fig. 6E), consistent with MC38 cell line with radiotherapy. And patients after radiation therapy with low expression of PRMT1 or PRMT5 had longer survival time (Fig. 6F).

CK8, scratch assay, and transwell invasion assay were utilized to determine whether knockdown or overexpression of PRMT1 or PRMT5 resulted in decreased or increased proliferation, migration, and invasion of cancer cells. Compared with control cells, cells with reduced PRMT1 or PRMT5 expression showed decreased proliferation, migration, and invasion. LUAD cell lines overexpressing PRMT1 or PRMT5 exhibited enhanced proliferation (Fig. 7A–B), migration (Fig. 7C–D), and invasion (Fig. 7E–F). In addition, the uncropped versions of western blotting in Fig. 2C–D, Fig. 5D, F, and I, and Fig. 6A, B, and E were provided as Supplementary files in Figs. S14–20.

Finally, our study revealed that PRMT1 and PRMT5 are potentially therapeutic targets in oncology and may facilitate radio-sensitization.

#### 4. Discussion

Methylation of arginine in proteins has been implicated in a variety of cellular processes, including signal transduction, gene transcription, DNA repair, mRNA splicing, cancer development, and metastasis [26,27]. Diverse cancer types frequently overexpress PRMTs, indicating their potential as effective therapeutic targets. The diagnostic and prognostic significance of PRMTs, as well as the mechanisms affecting the tumor immune microenvironment, especially in human LUAD, still need to be elucidated.

Because PRMT molecules share a common molecular structure and function, it is not feasible to investigate every molecule in this family thoroughly. For this reason, we have been focusing on PRMT1 and PRMT5 as representative molecules. In recent studies, protein arginine methylation has been linked to tumor immunotherapy [26]. An ADMA mark is deposited by PRMT1 at arginine 3 of histone H4 (H4R3me2a) [8]. Further, PRMT5, a Type II arginine methyltransferase, contributes to the development and progression of cancer [28–32]. cGAS-STING and NLR5 pathways are regulated by PRMT5, which play an important role in the presence of

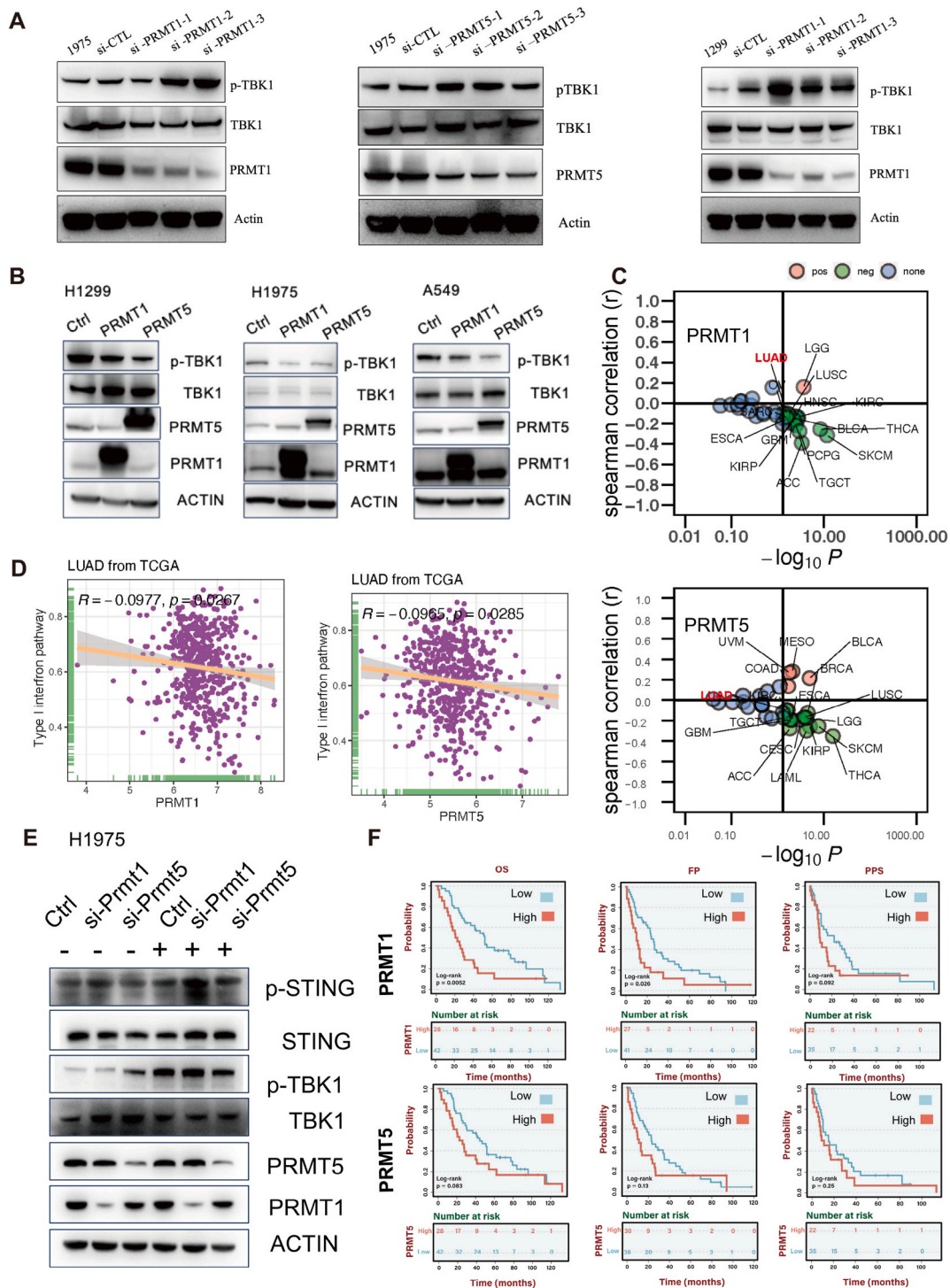
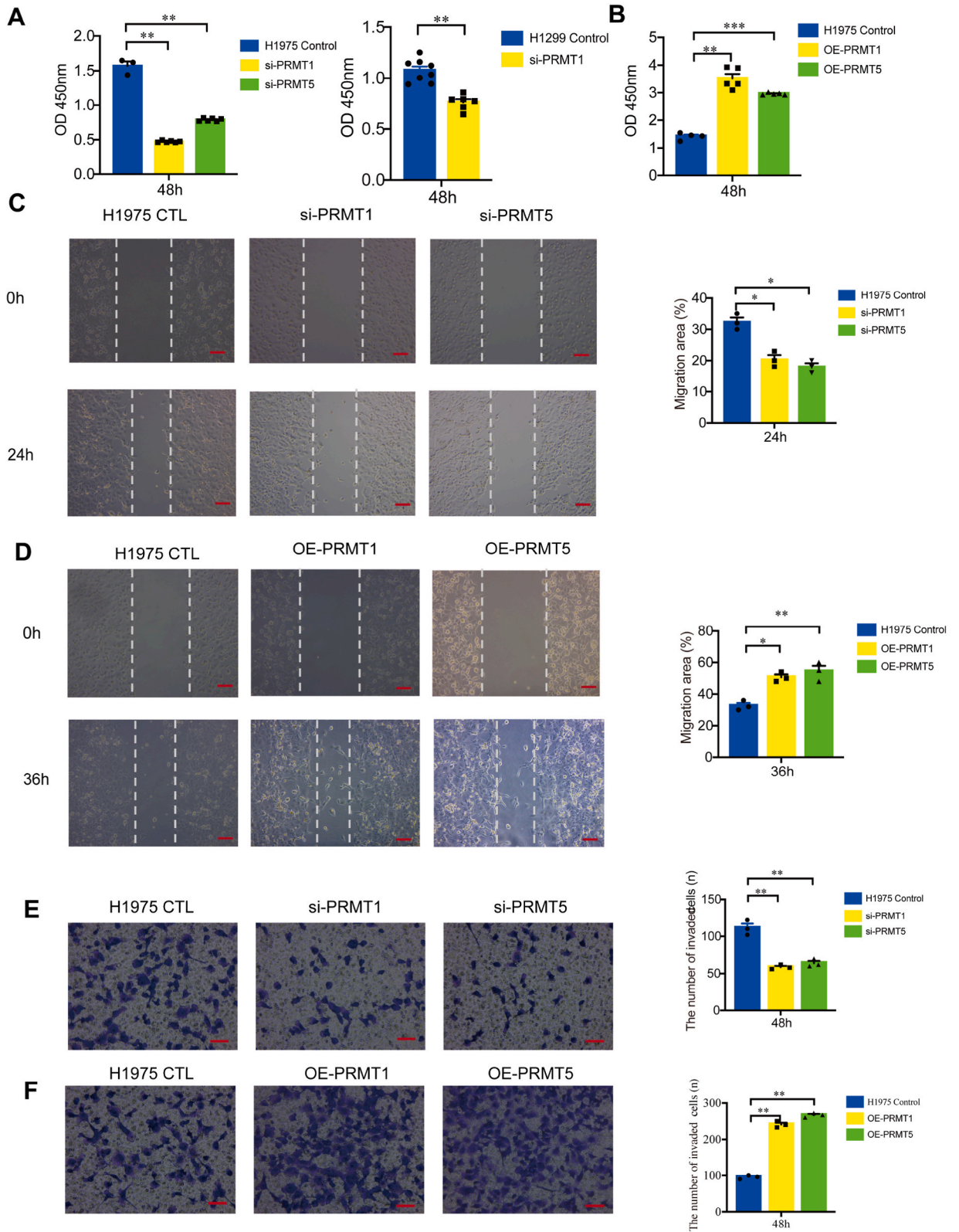


**Fig. 6.** Deficiency of intracellular PRMT1 or PRMT5 strongly activated the cGAS-STING pathway and improved the prognosis of LUAD patients with radiotherapy. A, p-TBK1 expression in the si-PRMT1 and si-PRMT5 LUAD tumor cell lines, including H1299 and H1975. B, p-TBK1 expression in Prmt1 or Prmt5 overexpressed LUAD tumor cells, including H1299, H1975, and A549. C, Correlation among PRMT1 (upper panel) and PRMT5 (lower panel) expression with Type I interferon pathway in TCGA pan-cancer cohorts. D, Correlation among PRMT1 (left panel) and PRMT5 (right panel) expression with Type I interferon pathway in TCGA LUAD cohort. E, p-STING and p-TBK1 expression in si-PRMT1 and si-PRMT5 LUAD H1975 cell line with or without IR. F, Association of PRMT1 or PRMT5 mRNA level with overall survival (OS), first-progression survival (FP), and post-progression survival (PPS) in TCGA LUAD cohort.



(caption on next page)

**Fig. 7.** The proliferation, migration and invasion ability in LUAD cell lines expressing PRMT1 or PRMT5. A–B, The results of cell counting kit-8 analysis of si-PRMT1 and si-PRMT5 (A), overexpressed PRMT1 and PRMT5 (B). C, The results of the scratch wound assay in Ctrl H1975 and si-PRMT1, and si-PRMT5 H1975 cell lines. Scale bar: 50  $\mu\text{m}$ . D, The results of the scratch wound assay in Ctrl H1975 and OE-PRMT1, and OE-PRMT5 H1975 cell lines. Scale bar: 50  $\mu\text{m}$ . E, The results of transwell invasion assay in Ctrl H1975 and si-PRMT1, and si-PRMT5 H1975 cell lines. Scale bar: 25  $\mu\text{m}$ . F, The results of transwell invasion assay in Ctrl H1975 and OE-PRMT1, and OE-PRMT5 H1975 cell lines. Scale bar: 25  $\mu\text{m}$ . ns,  $p > 0.05$ ; \*,  $p < 0.05$ ; \*\* $p < 0.01$ ; \*\*\* $p < 0.001$ ; \*\*\*\* $p < 0.0001$ .

anti-tumor immunity of melanoma [28]. It remains unclear how PRMT family genes function in lung cancer, and there is a dearth of research on the genes.

According to our findings, lung adenocarcinoma (LUAD) has elevated transcription and translational expression of PRMTs. PRMT1 and PRMT5 genes were investigated for their molecular expression, associated clinical characteristics, and genetic alterations, as well as their association with immune CD8<sup>+</sup> T cell infiltration CAF, TMB, MSI, and neoantigen loads across TCGA cancer types [33,34]. In addition to relating PRMT gene expression to prognosis, these results suggested that PRMT1 and PRMT5 may be considered significant diagnostic, prognostic biomarkers, as well as promising therapeutic targets for tumor immunotherapy. Multiple immunotherapy datasets for LUAD in the GEO database confirmed our hypothesis.

Intuitive and adaptive immunity are influenced by the IFN-I pathway, the most significant pathway triggering tumor immunity [35, 36]. Conventional chemotherapeutics, targeted anti-cancer agents, immunological adjuvants, and oncolytic viruses are only effective when the IFN-I signaling pathway is intact [37]. As an effective antitumor immunotherapy, IFN-I and related signaling pathways could be stimulated appropriately [38,39]. Based on our study, it appears that the IFN-I signaling pathway was activated by lower expression levels of PRMT1 or PRMT5 expression in both LUAD cell lines as well as MC38 cells. Interestingly, in non-small-cell lung carcinoma single-cell data, PRMT1 and PRMT5 expression were also negatively associated with inflammatory pathways. It is well known that the type I interferon pathway is the most familiar inflammatory pathway. We also found the infiltration of CD8<sup>+</sup> T cells was associated with low PRMT1 or PRMT5 expression. A powerful antitumor effect is stimulated by the type I interferon pathway when DC cells are activated to recruit CD8<sup>+</sup>T cells into the tumor microenvironment [12,35,40]. By activating type I interferon pathways through various mechanisms, radiotherapy can promote antitumor activity [41]. The improved survival of patients after radiotherapy suggests that radiotherapy may enhance the role of the IFN-I pathway, and we also utilized experiments *in vitro* and TCGA database analysis to verify this conclusion. Our research found that low expression of PRMT1 or PRMT5 may further enhance the therapeutic effect of radiotherapy owing to an improved IFN-I response for the first time. However, there is still much to learn about how PRMT1 or PRMT5 activate the type I interferon pathway to promote radiotherapeutic antitumor immunity and need further investigation.

Cell lines derived from human lung adenocarcinoma cells were found to display significantly impacted proliferation, migration, and invasion abilities when their expression levels of PRMT1 or PRMT5 were altered. According to previous studies, PRMT1 contributes to the proliferation, invasion, and metastasis of several types of cancer, including prostate cancer, colorectal cancer, pancreatic cancer, and renal cancer [42–47]. Furthermore, PRMT5 also promotes the proliferation, migration, and invasion of these cells [31, 48–51]. Our study compensates for the lack of evidence that PRMT1 or PRMT5 are involved in proliferation, migration, and invasion of human lung adenocarcinomas. Guozhen Gao evaluated the interaction between PRMT5 and PRMT1, finding that loss of PRMT1 sensitizes cells to PRMT5 inhibition, resulting in synergistic effects in small cells [52]. It appears that PRMT1 and PRMT5 are not acting alone, so future drug development may take into account their relationship.

## 5. Conclusion

The present study provided an in-depth analysis of PRMT1 and PRMT5 as potential immunological biomarkers for diagnosis and prognosis. High PRMT expression correlates directly with poor prognosis and immunosuppressive tumor microenvironment. The outcome after immunotherapy or radiotherapy is better for patients with LUAD who express low levels of PRMT1 or PRMT5. In LUAD, PRMT1 and PRMT5 may offer promising therapeutic targets for tumor immunotherapy and radiotherapy. Moreover, PRMT1 and PRMT5 confer radio-sensitization with the IFN-I interferon response through cGAS-STING pathway in LUAD cell lines. However, the specific mechanism still remains to be explored.

## Ethical approval and consent to participate

Not applicable.

## Funding

The study was supported by funds from the foundation of National Natural Science Foundation of China (82030082, 82002719 and 82172676), and the foundation of Natural Science Foundation of Shandong (ZR2020LZL014, ZR2021YQ52 and ZR2020LZL016). D-WC has received grants from the Young Elite Scientist Sponsorship Program by Cast (no. YESS20210137), China.

## Data availability statement

Data included in article/supp. material/referenced in article is open access in publicly available repositories.

## Consent for publication

Not applicable.

## CRedit authorship contribution statement

**Jia Wang:** Formal analysis, Validation, Visualization, Writing - original draft, Writing - review & editing. **Meng Wu:** Data curation, Methodology. **Jujie Sun:** Validation. **Minxin Chen:** Investigation, Methodology. **Zengfu Zhang:** Software. **Jinming Yu:** Funding acquisition, Methodology. **Dawei Chen:** Funding acquisition, Investigation.

## Declaration of competing interest

The authors declare that they have no known competing financial interests or personal relationships that could have appeared to influence the work reported in this paper.

## Acknowledgments

We appreciate Dr. Wenlong Li for kind help in manuscript editing.

## Appendix A. Supplementary data

Supplementary data to this article can be found online at <https://doi.org/10.1016/j.heliyon.2023.e22088>.

## List of Abbreviations

ACC	Adrenocortical Cancer
ADMA	asymmetric dimethylarginine
AML	Acute Myeloid Leukemia
AUC	area under the curve
BEST	Biomarker Exploration of Solid Tumor
BLCA	Bladder Cancer
BRCA	Breast Cancer
CAF	cancer-associated fibroblast
CESC	Cervical Cancer
CHOL	Cholangiocarcinoma
CI	confidence interval
COAD	Colon Cancer
DFS	disease-free survival
DLBC	Large B-cell Lymphoma
ESCA	Esophageal Cancer
FPKM	fragments per kilobase of exon per million mapped fragments
FPS	first-progression survival
GBM	Glioblastoma
GTE <sub>x</sub>	Genotype-Tissue Expression
HBE	human bronchial epithelial cells
HNSC	Head and Neck Cancer
HPA	the Human Protein Atlas
HR	hazard ratio
IFN-I	type I interferon
ISGs	interferon-stimulated genes
KEGG	Kyoto Encyclopedia of Genes and Genomes
KICH	Kidney Chromophobe
KIRC	Kidney Clear Cell Carcinoma
KIRP	Kidney Papillary Cell Carcinoma
LGG	lower grade glioma
LIHC	Liver Cancer
LUAD	lung adenocarcinoma
LUSC	Lung Squamous Cell Carcinoma
MESO	Mesothelioma
MMA	mono-methylarginine
MSI	microsatellite instability

OS	overall survival
OV	Ovarian Serous Cystadenocarcinoma
PAAD	Pancreatic Cancer
PCPG	Pheochromocytoma & Paraganglioma
PPS	post-progression survival
PRAD	Prostate Adenocarcinoma
PRMT	protein arginine methyltransferase
READ	Rectum adenocarcinoma
ROC	receiver operating characteristic
SARC	Sarcoma; SDMA, symmetric dimethylarginine
SKCM	Skin Cutaneous Melanoma
STAD	Stomach adenocarcinoma
TCGA	The Cancer Genome Atlas
TGCT	Testicular Germ Cell Tumors
THCA	Thyroid carcinoma
THYM	Thymoma
TIME	tumor immune microenvironment
TMB	tumor mutational burden
UALCAN	The University of Alabama at Birmingham CANcer data analysis Portal
UCEC	Uterine Corpus Endometrial Carcinoma
UCS	Uterine Carcinosarcoma

## References

- [1] H. Sung, J. Ferlay, R.L. Siegel, M. Laversanne, I. Soerjomataram, A. Jemal, F. Bray, Global cancer statistics 2020: GLOBOCAN estimates of incidence and mortality worldwide for 36 cancers in 185 countries, *CA, Cancer J. Clin.* 71 (2021) 209–249, <https://doi.org/10.3322/caac.21660>.
- [2] M. Reck, J. Remon, M.D. Hellmann, First-line immunotherapy for non-small-cell lung cancer, *J. Clin. Oncol. Off. J. Am. Soc. Clin. Oncol.* 40 (2022) 586–597, <https://doi.org/10.1200/JCO.21.01497>.
- [3] J.W. Hwang, Y. Cho, G.-U. Bae, S.-N. Kim, Y.K. Kim, Protein arginine methyltransferases: promising targets for cancer therapy, *Exp. Mol. Med.* 53 (2021) 788–808, <https://doi.org/10.1038/s12276-021-00613-y>.
- [4] R.S. Blanc, S. Richard, Arginine methylation: the coming of age, *Mol. Cell.* 65 (2017) 8–24, <https://doi.org/10.1016/j.molcel.2016.11.003>.
- [5] A. Fedoriv, L. Shi, S. O'Brien, K.N. Smitheman, Y. Wang, J. Hou, C. Sherk, S. Rajapurkar, J. Lario, L.J. Williams, C. Xu, G. Han, Q. Feng, M.T. Bedford, L. Wang, O. Barbash, R.G. Kruger, P. Hwu, H.P. Mohammad, W. Peng, Inhibiting type I arginine methyltransferase activity promotes T cell-mediated antitumor immune responses, *Cancer Immunol. Res.* 10 (2022) 420–436, <https://doi.org/10.1158/2326-6066.CIR-21-0614>.
- [6] J. Liu, X. Bu, C. Chu, X. Dai, J.M. Asara, P. Sicinski, G.J. Freeman, W. Wei, PRMT1 mediated methylation of cGAS suppresses anti-tumor immunity, *Nat. Commun.* 14 (2023) 2806, <https://doi.org/10.1038/s41467-023-38443-3>.
- [7] W. Dai, J. Zhang, S. Li, F. He, Q. Liu, J. Gong, Z. Yang, Y. Gong, F. Tang, Z. Wang, C. Xie, Protein arginine methylation: an emerging modification in cancer immunity and immunotherapy, *Front. Immunol.* 13 (2022), 865964, <https://doi.org/10.3389/fimmu.2022.865964>.
- [8] Q. Wu, M. Schapira, C.H. Arrowsmith, D. Barsyte-Lovejoy, Protein arginine methylation: from enigmatic functions to therapeutic targeting, *Nat. Rev. Drug Discov.* 20 (2021) 509–530, <https://doi.org/10.1038/s41573-021-00159-8>.
- [9] E. Guccione, S. Richard, The regulation, functions and clinical relevance of arginine methylation, *Nat. Rev. Mol. Cell Biol.* 20 (2019) 642–657, <https://doi.org/10.1038/s41580-019-0155-x>.
- [10] Y. Hou, H. Liang, E. Rao, W. Zheng, X. Huang, L. Deng, Y. Zhang, X. Yu, M. Xu, H. Mauceri, A. Arina, R.R. Weichselbaum, Y.-X. Fu, Non-canonical NF- $\kappa$ B antagonizes STING sensor-mediated DNA sensing in radiotherapy, *Immunity* 49 (2018) 490–503.e4, <https://doi.org/10.1016/j.immuni.2018.07.008>.
- [11] T.F. Gajewski, L. Corrales, New perspectives on type I IFNs in cancer, *Cytokine Growth Factor Rev.* 26 (2015) 175–178, <https://doi.org/10.1016/j.cytogfr.2015.01.001>.
- [12] F. Zhang, S. Manna, L.M. Pop, Z.J. Chen, Y.-X. Fu, R. Hannan, Type I interferon response in radiation-induced anti-tumor immunity, *Semin. Radiat. Oncol.* 30 (2020) 129–138, <https://doi.org/10.1016/j.semradonc.2019.12.009>.
- [13] B.C. Burnette, H. Liang, Y. Lee, L. Chlewicki, N.N. Khodarev, R.R. Weichselbaum, Y.-X. Fu, S.L. Auh, The efficacy of radiotherapy relies upon induction of type I interferon-dependent innate and adaptive immunity, *Cancer Res.* 71 (2011) 2488–2496, <https://doi.org/10.1158/0008-5472.CAN-10-2820>.
- [14] A. Sistigu, T. Yamazaki, E. Vacchelli, K. Chaba, D.P. Enot, J. Adam, I. Vitale, A. Goubar, E.E. Baracco, C. Remédios, L. Fend, D. Hannani, L. Aymeric, Y. Ma, M. Niso-Santano, O. Kepp, J.L. Schultze, T. Tüting, F. Belardelli, L. Bracci, V. La Sorsa, G. Ziccheddu, P. Sestili, F. Urbani, M. Delorenzi, M. Lacroix-Triki, V. Quidville, R. Conforti, J.-P. Spano, L. Pusztai, V. Poirier-Colame, S. Delalogue, F. Penault-Llorca, S. Ladoire, L. Arnould, J. Cyrt, M.-C. Dessoliers, A. Eggermont, M.E. Bianchi, M. Pittet, C. Engblom, C. Pfirschke, X. Prévile, G. Uzé, R.D. Schreiber, M.T. Chow, M.J. Smyth, E. Proietti, F. André, G. Kroemer, L. Zitvogel, Cancer cell-autonomous contribution of type I interferon signaling to the efficacy of chemotherapy, *Nat. Med.* 20 (2014) 1301–1309, <https://doi.org/10.1038/nm.3708>.
- [15] GTEx Consortium, The genotype-tissue expression (GTEx) project, *Nat. Genet.* 45 (2013) 580–585, <https://doi.org/10.1038/ng.2653>.
- [16] E. Cerami, J. Gao, U. Dogrusoz, B.E. Gross, S.O. Sumer, B.A. Aksoy, A. Jacobsen, C.J. Byrne, M.L. Heuer, E. Larsson, Y. Antipin, B. Reva, A.P. Goldberg, C. Sander, N. Schultz, The cBio cancer genomics portal: an open platform for exploring multidimensional cancer genomics data, *Cancer Discov.* 2 (2012) 401–404, <https://doi.org/10.1158/2159-8290.CD-12-0095>.
- [17] D.S. Chandrashekar, S.K. Karthikeyan, P.K. Korla, H. Patel, A.R. Shovon, M. Athar, G.J. Netto, Z.S. Qin, S. Kumar, U. Manne, C.J. Creighton, S. Varambally, UALCAN: an update to the integrated cancer data analysis platform, *Neoplasia* 25 (2022) 18–27, <https://doi.org/10.1016/j.neo.2022.01.001>.
- [18] D.S. Chandrashekar, B. Bashel, S.A.H. Balasubramanya, C.J. Creighton, I. Ponce-Rodriguez, B.V.S.K. Chakravarthi, S. Varambally, UALCAN: a portal for facilitating tumor subgroup gene expression and survival analyses, *Neoplasia* 19 (2017) 649–658, <https://doi.org/10.1016/j.neo.2017.05.002>.
- [19] K. Nakamura, M.J. Smyth, Myeloid immunosuppression and immune checkpoints in the tumor microenvironment, *Cell. Mol. Immunol.* 17 (2020) 1–12, <https://doi.org/10.1038/s41423-019-0306-1>.
- [20] K. Li, H. Shi, B. Zhang, X. Ou, Q. Ma, Y. Chen, P. Shu, D. Li, Y. Wang, Myeloid-derived suppressor cells as immunosuppressive regulators and therapeutic targets in cancer, *Signal Transduct. Targeted Ther.* 6 (2021) 362, <https://doi.org/10.1038/s41392-021-00670-9>.

- [21] D. Lambrechts, E. Wauters, B. Boeckx, S. Aibar, D. Nittner, O. Burton, A. Bassez, H. Decaluwé, A. Pircher, K. Van den Eynde, B. Weynand, E. Verbeken, P. De Leyn, A. Liston, J. Vansteenkiste, P. Carmeliet, S. Aerts, B. Thienpont, Phenotype molding of stromal cells in the lung tumor microenvironment, *Nat. Med.* 24 (2018) 1277–1289, <https://doi.org/10.1038/s41591-018-0096-5>.
- [22] K.-T. Kim, H.-W. Lee, H.-O. Lee, S.-C. Kim, Y.-J. Seo, W. Chung, H.-H. Eum, D.-H. Nam, J. Kim, K.-M. Joo, W.-Y. Park, Single-cell mRNA sequencing identifies subclonal heterogeneity in anti-cancer drug responses of lung adenocarcinoma cells, *Genome Biol.* 16 (2015) 127, <https://doi.org/10.1186/s13059-015-0692-3>.
- [23] C. Han, Z. Liu, Y. Zhang, A. Shen, C. Dong, A. Zhang, C. Moore, Z. Ren, C. Lu, X. Cao, C.-L. Zhang, J. Qiao, Y.-X. Fu, Tumor cells suppress radiation-induced immunity by hijacking caspase 9 signaling, *Nat. Immunol.* 21 (2020) 546–554, <https://doi.org/10.1038/s41590-020-0641-5>.
- [24] M. Wang, Y. Huang, M. Chen, W. Wang, F. Wu, T. Zhong, X. Chen, F. Wang, Y. Li, J. Yu, M. Wu, D. Chen, Inhibition of tumor intrinsic BANF1 activates antitumor immune responses via cGAS-STING and enhances the efficacy of PD-1 blockade, *J. Immunother. Cancer.* 11 (2023), e007035, <https://doi.org/10.1136/jitc-2023-007035>.
- [25] Y. Yang, M. Wu, D. Cao, C. Yang, J. Jin, L. Wu, X. Hong, W. Li, L. Lu, J. Li, X. Wang, X. Meng, Z. Zhang, J. Cheng, Y. Ye, H. Xiao, J. Yu, L. Deng, ZBP1-MLKL necroptotic signaling potentiates radiation-induced antitumor immunity via intratumoral STING pathway activation, *Sci. Adv.* 7 (2021), eabf6290, <https://doi.org/10.1126/sciadv.abf6290>.
- [26] S.K. Tewary, Y.G. Zheng, M.-C. Ho, Protein arginine methyltransferases: insights into the enzyme structure and mechanism at the atomic level, *Cell. Mol. Life Sci. CMLS* 76 (2019) 2917–2932, <https://doi.org/10.1007/s00018-019-03145-x>.
- [27] J. Xu, S. Richard, Cellular pathways influenced by protein arginine methylation: implications for cancer, *Mol. Cell.* 81 (2021) 4357–4368, <https://doi.org/10.1016/j.molcel.2021.09.011>.
- [28] H. Kim, H. Kim, Y. Feng, Y. Li, H. Tamiya, S. Tocci, Z.A. Ronai, PRMT5 control of cGAS-STING and NLR5 pathways defines melanoma response to antitumor immunity, *Sci. Transl. Med.* 12 (2020), <https://doi.org/10.1126/scitranslmed.aaz5683> eaz5683.
- [29] L.C. Litzler, A. Zahn, A.P. Meli, S. Hébert, A.-M. Patenaude, S.P. Methot, A. Sprumont, T. Bois, D. Kitamura, S. Costantino, I.L. King, C.L. Kleinman, S. Richard, J. M. Di Noia, PRMT5 is essential for B cell development and germinal center dynamics, *Nat. Commun.* 10 (2019) 22, <https://doi.org/10.1038/s41467-018-07884-6>.
- [30] Y. Luo, Y. Gao, W. Liu, Y. Yang, J. Jiang, Y. Wang, W. Tang, S. Yang, L. Sun, J. Cai, X. Guo, S. Takahashi, K.W. Krausz, A. Qu, L. Chen, C. Xie, F.J. Gonzalez, Myelocytomatosis-protein arginine N-methyltransferase 5 Axis defines the tumorigenesis and immune response in hepatocellular carcinoma, *Hepatol. Baltim. Md.* 74 (2021) 1932–1951, <https://doi.org/10.1002/hep.31864>.
- [31] Y. Jiang, Y. Yuan, M. Chen, S. Li, J. Bai, Y. Zhang, Y. Sun, G. Wang, H. Xu, Z. Wang, Y. Zheng, H. Nie, PRMT5 disruption drives antitumor immunity in cervical cancer by reprogramming T cell-mediated response and regulating PD-L1 expression, *Theranostics* 11 (2021) 9162–9176, <https://doi.org/10.7150/thno.59605>.
- [32] R. Hu, B. Zhou, Z. Chen, S. Chen, N. Chen, L. Shen, H. Xiao, Y. Zheng, PRMT5 inhibition promotes PD-L1 expression and immuno-resistance in lung cancer, *Front. Immunol.* 12 (2021), 722188, <https://doi.org/10.3389/fimmu.2021.722188>.
- [33] S. Bagchi, R. Yuan, E.G. Engleman, Immune checkpoint inhibitors for the treatment of cancer: clinical impact and mechanisms of response and resistance, *Annu. Rev. Pathol.* 16 (2021) 223–249, <https://doi.org/10.1146/annurev-pathol-042020-042741>.
- [34] X. Ren, L. Zhang, Y. Zhang, Z. Li, N. Siemers, Z. Zhang, Insights gained from single-cell analysis of immune cells in the tumor microenvironment, *Annu. Rev. Immunol.* 39 (2021) 583–609, <https://doi.org/10.1146/annurev-immunol-110519-071134>.
- [35] L.M. Snell, T.L. McGaha, D.G. Brooks, Type I interferon in chronic virus infection and cancer, *Trends Immunol.* 38 (2017) 542–557, <https://doi.org/10.1016/j.it.2017.05.005>.
- [36] L. Zitvogel, L. Galluzzi, O. Kepp, M.J. Smyth, G. Kroemer, Type I interferons in anticancer immunity, *Nat. Rev. Immunol.* 15 (2015) 405–414, <https://doi.org/10.1038/nri3845>.
- [37] O. Takeuchi, S. Akira, Pattern recognition receptors and inflammation, *Cell* 140 (2010) 805–820, <https://doi.org/10.1016/j.cell.2010.01.022>.
- [38] L. Bracci, A. Sisti, E. Proietti, F. Moschella, The added value of type I interferons to cytotoxic treatments of cancer, *Cytokine Growth Factor Rev.* 36 (2017) 89–97, <https://doi.org/10.1016/j.cytogfr.2017.06.008>.
- [39] J. Zheng, J. Mo, T. Zhu, W. Zhuo, Y. Yi, S. Hu, J. Yin, W. Zhang, H. Zhou, Z. Liu, Comprehensive elaboration of the cGAS-STING signaling axis in cancer development and immunotherapy, *Mol. Cancer* 19 (2020) 133, <https://doi.org/10.1186/s12943-020-01250-1>.
- [40] Y. Liang, R. Hannan, Y.-X. Fu, Type I IFN activating type I dendritic cells for antitumor immunity, *Clin. Cancer Res. Off. J. Am. Assoc. Cancer Res.* 27 (2021) 3818–3824, <https://doi.org/10.1158/1078-0432.CCR.20-2564>.
- [41] L. Deng, H. Liang, M. Xu, X. Yang, B. Burnette, A. Arina, X.-D. Li, H. Mauceri, M. Beckett, T. Darga, X. Huang, T.F. Gajewski, Z.J. Chen, Y.-X. Fu, R. Weichselbaum, STING-dependent cytosolic DNA sensing promotes radiation-induced type I interferon-dependent antitumor immunity in immunogenic tumors, *Immunity* 41 (2014) 843–852, <https://doi.org/10.1016/j.immuni.2014.10.019>.
- [42] J. Wang, C. Wang, P. Xu, X. Li, Y. Lu, D. Jin, X. Yin, H. Jiang, J. Huang, H. Xiong, F. Ye, J. Jin, Y. Chen, Y. Xie, Z. Chen, H. Ding, H. Zhang, R. Liu, H. Jiang, K. Chen, Z. Yao, C. Luo, Y. Huang, Y. Zhang, J. Zhang, PRMT1 is a novel molecular therapeutic target for clear cell renal cell carcinoma, *Theranostics* 11 (2021) 5387–5403, <https://doi.org/10.7150/thno.42345>.
- [43] Z. Li, D. Wang, X. Chen, W. Wang, P. Wang, P. Hou, M. Li, S. Chu, S. Qiao, J. Zheng, J. Bai, PRMT1-mediated EZH2 methylation promotes breast cancer cell proliferation and tumorigenesis, *Cell Death Dis.* 12 (2021) 1080, <https://doi.org/10.1038/s41419-021-04381-5>.
- [44] X.-K. Yin, Y.-L. Wang, F. Wang, W.-X. Feng, S.-M. Bai, W.-W. Zhao, L.-L. Feng, M.-B. Wei, C.-L. Qin, F. Wang, Z.-L. Chen, H.-J. Yi, Y. Huang, P.-Y. Xie, T. Kim, Y.-N. Wang, J.-W. Hou, C.-W. Li, Q. Liu, X.-J. Fan, M.-C. Hung, X.-B. Wan, PRMT1 enhances oncogenic arginine methylation of NONO in colorectal cancer, *Oncogene* 40 (2021) 1375–1389, <https://doi.org/10.1038/s41388-020-01617-0>.
- [45] B. Yao, T. Gui, X. Zeng, Y. Deng, Z. Wang, Y. Wang, D. Yang, Q. Li, P. Xu, R. Hu, X. Li, B. Chen, J. Wang, K. Zen, H. Li, M.J. Davis, M.J. Herold, H.-F. Pan, Z.-W. Jiang, D.C.S. Huang, M. Liu, J. Ju, Q. Zhao, PRMT1-mediated H4R3me2a recruits SMARCA4 to promote colorectal cancer progression by enhancing EGFR signaling, *Genome Med.* 13 (2021) 58, <https://doi.org/10.1186/s13073-021-00871-5>.
- [46] Z. Li, D. Wang, J. Lu, B. Huang, Y. Wang, M. Dong, D. Fan, H. Li, Y. Gao, P. Hou, M. Li, H. Liu, Z.-Q. Pan, J. Zheng, J. Bai, Methylation of EZH2 by PRMT1 regulates its stability and promotes breast cancer metastasis, *Cell Death Differ.* 27 (2020) 3226–3242, <https://doi.org/10.1038/s41418-020-00615-9>.
- [47] C. Song, T. Chen, L. He, N. Ma, J.-A. Li, Y.-F. Rong, Y. Fang, M. Liu, D. Xie, W. Lou, PRMT1 promotes pancreatic cancer growth and predicts poor prognosis, *Cell. Oncol. Dordr.* 43 (2020) 51–62, <https://doi.org/10.1007/s13402-019-00435-1>.
- [48] S. Yin, L. Liu, C. Brobbey, V. Palanisamy, L.E. Ball, S.K. Olsen, M.C. Ostrowski, W. Gan, PRMT5-mediated arginine methylation activates AKT kinase to govern tumorigenesis, *Nat. Commun.* 12 (2021) 3444, <https://doi.org/10.1038/s41467-021-23833-2>.
- [49] P. Sachamitr, J.-C. Ho, F.E. Ciamponi, W. Ba-Alawi, F.J. Coutinho, P. Guilhamon, M.M. Kushida, F.M.G. Cavalli, L. Lee, N. Rastegar, V. Vu, M. Sánchez-Osuna, J. Coulombe-Huntington, E. Kanshin, H. Whetstone, M. Durand, P. Thibault, K. Hart, M. Mangos, J. Veyhl, W. Chen, N. Tran, B.-C. Duong, A.M. Aman, X. Che, X. Lan, O. Whitley, O. Zaslaver, D. Barsyte-Lovejoy, L.M. Richards, I. Restall, A. Caudy, H.L. Röst, Z.Q. Bonday, M. Bernstein, S. Das, M.D. Cusimano, J. Spears, G.D. Bader, T.J. Pugh, M. Tyers, M. Lupien, B. Haibe-Kains, H. Artee Luchman, S. Weiss, K.B. Massier, P. Prinos, C.H. Arrowsmith, P.B. Dirks, PRMT5 inhibition disrupts splicing and stemness in glioblastoma, *Nat. Commun.* 12 (2021) 979, <https://doi.org/10.1038/s41467-021-21204-5>.
- [50] L. Yang, D.-W. Ma, Y.-P. Cao, D.-Z. Li, X. Zhou, J.-F. Feng, J. Bao, PRMT5 functionally associates with EZH2 to promote colorectal cancer progression through epigenetically repressing CDKN2B expression, *Theranostics* 11 (2021) 3742–3759, <https://doi.org/10.7150/thno.53023>.
- [51] N. Wang, H. Yan, D. Wu, Z. Zhao, X. Chen, Q. Long, C. Zhang, X. Wang, W. Deng, X. Liu, PRMT5/Wnt4 axis promotes lymph-node metastasis and proliferation of laryngeal carcinoma, *Cell Death Dis.* 11 (2020) 864, <https://doi.org/10.1038/s41419-020-03064-x>.
- [52] G. Gao, L. Zhang, O.D. Villarreal, W. He, D. Su, E. Bedford, P. Moh, J. Shen, X. Shi, M.T. Bedford, H. Xu, PRMT1 loss sensitizes cells to PRMT5 inhibition, *Nucleic Acids Res.* 47 (2019) 5038–5048, <https://doi.org/10.1093/nar/gkz200>.